LA-UR-06-3018, Structural Control and Health Monitoring, Vol 15, No.1 pp.43-63, 2008:

The Use of Macro-Fiber Composites for Pipeline Structural Health Assessment

Andrew B. Thien, Heather C. Chiamori, Jeff T. Ching, Jeannette R. Wait, Gyuhae Park

The Engineering Institute
Los Alamos National Laboratory
Los Alamos, NM 87545

Total number of pages = 42 including figures and this page

Total number of figures = 11

Proofs are to be sent to:

Gyuhae Park, Ph.D.
The Engineering Institute
Mail Stop T001
Los Alamos National Laboratory
Los Alamos, NM 87545

Phone: 505-663-5335
Fax: 505-663-5225
e-mail: gpark@lanl.gov

The Use of Macro-Fiber Composites for Pipeline Structural Health Assessment

Andrew B. Thien, Heather C. Chiamori, Jeff T. Ching, Jeannette R. Wait, Gyuhae Park*

The Engineering Institute
Los Alamos National Laboratory
Los Alamos, NM 87545

ABSTRACT

Pipeline structures are susceptible to cracks, corrosion, and other aging defects. If left undetected, these forms of damage can lead to the failure of the pipeline system, which may have catastrophic consequences. Most current forms of health monitoring for pipeline systems involve nondestructive evaluation (NDE) techniques. These techniques require sophisticated instruments and direct access to the structure, which is not always possible for civil pipeline applications. This research proposes the use of Macro-fiber composite (MFC) transducers for real-time structural health monitoring in pipeline systems. In particular, we propose the coupled implementation of impedance based and Lamb wave based methods that are simultaneously used to accurately determine the health of a pipeline network. The self-sensing impedance methods are used to detect structural damage occurring at pipeline connection joints, while the Lamb wave propagation measurements identify cracks and corrosion along the surface and through the wall thickness of the pipe structure. Both methods utilize the same MFC active sensors, which are flexible, durable, relatively inexpensive, and can be permanently bonded to the surface of a pipe during installation. Therefore, measurements for damage identification can be performed at any time, even while the system is in operation. Based on the success of this study, guidelines

* Author to whom correspondence should be addressed. Email:gpark@lanl.gov

are outlined for the full-scale development of a low cost, active-sensing based SHM system suitable for pipeline applications.

Nomenclature

a	geometric constant of material of piezoelectric materials
d_{3x}	sensor coupling constant at a neutral state
$F(m,n)$	flexural non-axially symmetric modes with harmonic number of circumferential variation and index counter
$L(m,n)$	Longitudinal axially symmetric modes with index counter
$T(m,n)$	torsional axially symmetric modes with index counter
$Y(\omega)$	electrical admittance
Y_{xx}^{E}	complex Young's modulus with a zero electric field
Z_a	sensor mechanical impedance
Z_s	host structure mechanical impedance
ε_{33}^{T}	dielectric constant at a neutral state
ρ	Correlation coefficient
$Z_{i,1}$	Baseline impedance data at frequency i
$Z_{i,2}$	Compared impedance data at frequency i
$\overline{Z}_1$	Mean of signal
σ	Standard deviations

1. INTRODUCTION

The United States obtains approximately 65% of its total energy consumption from petroleum products, and millions of miles of pipelines exist to transport this energy resource [1]. Several issues emphasize the importance of developing and implementing a real-time, structural health monitoring (SHM) system for pipeline structures. First, the ability to quickly and accurately

evaluate the condition of a pipeline structure after a natural disaster, such as an earthquake, is critical to uninterrupted plant or facility operation as well as maintaining the safety of workers and nearby residents. Delays in the assessment of a potentially damaged pipeline could result in fire hazards caused by the rupture of gas pipelines or the shutdown of critical supply lines. Another reason to pursue a robust pipeline health monitoring system involves the reduction of operational and maintenance costs. Furthermore, several documented gas pipeline accidents have resulted because of difficulties with detecting pipeline damage [2,3].

Most current forms of health assessment for pipeline systems involve nondestructive evaluation (NDE) techniques [4, 5]. These techniques often require a pipeline system to be taken out of operation at regularly scheduled intervals so that a technician can perform a prescribed NDE measurement. Such a measurement also requires direct access to the pipe's exterior or interior surface. This access may require excavation if the pipe is underground and the removal of insulating layers when present. However, shutting down an entire plant or a section of a supply line to perform the maintenance is expensive, time-consuming, and reduces plant efficiency and production capabilities. Furthermore, these NDE techniques hold limited potential for real-time assessment immediately after a natural disaster, such as an earthquake.

If a well designed, structural health monitoring system were in operation, it is evident that one could reduce the maintenance cost and avoid catastrophic failure associated with pipeline structures. A promising technology for pipeline structural health monitoring investigated in this study involves the use of piezoelectric materials, such as Lead Zirconate Titanate (PZT). The electromechanical coupling effect of PZT transducers establishes a direct correlation between the

electrical and mechanical response of the transducer. As a result, a PZT patch experiences a mechanical strain when an electric field is applied, and conversely, a PZT material produces an electric charge when stressed mechanically. The coupling property allows PZT transducers to perform both actuation and sensing in a structural health monitoring system. When bonded to a structure, the PZT patch can be used to excite the system at high frequencies, utilizing the high-bandwidth capability of the PZT material, and then measure corresponding structural responses. Examples of documented success using PZT active sensors in the areas of SHM are impedance-based structural health monitoring methods [6,7,8], Lamb wave propagations [9,10], and the integrated use of these two methods [11,12]. Here the integrated use referrers to the use of each method at a time to improve damage detection capability. It does not necessary mean the full integration of hardware and software of two techniques.

The advantages of using PZT for SHM include low cost, light-weight, low-power consumption, non-intrusive, and high bandwidth that allow the detection of incipient-type damage. In this study, piezoelectric Macro-Fiber Composite (MFC) transducers are used for the development of a real-time, low cost, structural health monitoring system for pipeline structures. Additional advantages are obtained through the use of MFC patches, including high flexibility and extreme durability compared to their piezoceramic counterpart [13,14,15]. The flexibility of MFC patches is particularly useful to pipeline monitoring because the curved surface of the pipe may be used as an application site. The MFC transducers can be permanently bonded to the surface of a pipe during installation. Therefore, measurements for damage identification can be performed at any time, even while the system is still in operation.

In this study, the dual use of the MFC transducer was experimentally employed to utilize both impedance methods and Lamb wave propagations. Contrary to the previous study of the dual use of PZT active sensors [7], which proposes the detection of near-field and far-field damage using these two damage identification schemes, this method utilizes the different sensitivity of each method to the different types of damage. In particular, the self-sensing impedance methods are used to detect structural damage occurring at pipeline connection joints, while the Lamb wave propagation measurements identify cracks and corrosion along the surface and through the thickness of the pipe structure. This coupled approach also provides a certain advantage over traditional NDE techniques applied to pipeline structures because the NDE methods are only designed to identify cracks or corrosion in the main body of pipelines. The importance of monitoring connections and joints which are used to connect segmented pipelines should not be overlooked because this interface can be the most critical source of failure of the pipelines. It has been reported that approximately 70% of all mechanical failures are caused by fastener failure [16]. Furthermore, during an earthquake, significant seismic loadings can stress the joint beyond its yield or buckling capacity resulting in failures, while the main body of the pipe remains elastic [17].

This paper describes the performance of the proposed SHM technique in detecting real-time damage on a sample pipeline structure. Several conditions were imposed to simulate real-time damage, and the capability of the technique in tracking and monitoring the integrity of an industrial pipeline has been demonstrated. The theory behind this technique and the experimental investigations are presented in the following sections.

2. BACKGROUND

2.1 Impedance Method

Based on the work of Sun, et al. [18], the impedance-based monitoring technique can be used to monitor real-time changes in the mechanical impedance of a structure. Compared with initial measurements, a damaged structure will exhibit changes in its stiffness and damping characteristics, which affect its mechanical impedance. Because direct measurements of the mechanical impedance of a structure are difficult to obtain, the electromechanical coupling effect of PZT materials is utilized. Any damage to a host structure will result in changes to its mechanical impedance, which will be observed by changes in the electrical impedance of the PZT materials. In order to ensure the high sensitivity to small defects in a structure, the impedance measurements are usually made at higher frequency ranges, typically greater than 30 kHz.

In this experiment, the MFC patch acts as both an actuator and a sensor when obtaining the impedance signature from a structure. An alternating electric field is applied to the MFC patch, creating high frequency excitations in the host structure. At high frequencies, a dynamic response of the host structure is generated only in an area local to the patch. This local response is then measured by the MFC sensor as an electrical response. The relationship between the host structure's mechanical impedance and the electrical impedance of the MFC patch is represented by the following equation [18]:

$$Y(\omega) = \frac{I}{V} = i\omega a\left(\bar{\varepsilon}_{33}^{\ T} - \frac{Z_s(\omega)}{Z_s(\omega)+Z_a(\omega)} d_{3x}^2 \hat{Y}_{xx}^{\ E}\right) \tag{1}$$

where Y is the electrical admittance or the inverse of the electrical impedance, a is the PZT material's geometric constant, $\varepsilon_{33}^{\ T}$ is the dielectric constant at a neutral state, Z_a is the PZT's

mechanical impedance, Z_s is the host structure's mechanical impedance, d_{3x} is the PZT coupling constant at a neutral state, and Y_{xx}^{E} is the PZT's complex Young's modulus with a zero electric field. Because all parameters except Z_s, the host structure's mechanical impedance, are properties of the PZT material, only the mechanical impedance of a structure uniquely defines the electrical impedance of the PZT transducer. As a result, the electrical impedance signature of the PZT transducer is affected by changes in the host structure's mechanical impedance. Hence, by monitoring the electrical impedance and comparing this to a baseline impedance measurement, we can determine when structural damage has either occurred or is imminent. In addition, impedance measurements also have the potential to perform in-situ active sensor diagnosis that performs in-situ monitoring of the operational status of piezoelectric materials used for sensors and actuators in SHM applications. The basis of the sensor diagnostic procedure is to track the changes in the capacitive value of piezoelectric materials, which is manifested in the imaginary part of the measured electrical admittances [19,20]. For additional information regarding impedance methods, refer to [6,7,8].

For the impedance method, a scalar damage metric is used to interpret and quantify the variations of measured responses. The damage metrics that were used in the previous studies are correlation coefficients or the Root-Mean-Square-Deviation [6]. The degree of linear relationship between baselines and in-question measurements can be assessed with the damage metrics. For the impedance method, only the real component of the impedance measurement is considered because of its greater sensitivity to damage [6].

2.2 Lamb Wave propagation Method

Much effort has been directed toward the use of Lamb wave propagation as a structural health monitoring tool in plates, hollow cylinders, such as pipes, and other complex structures. Lamb waves are useful for corrosion detection because the waves are sensitive to surface and internal damage and propagate over long distances, which is especially useful for pipe structures [4]. Lamb waves are mechanical waves that have wavelengths on the same order of magnitude as the thickness of a structure and occur as an infinite number of discrete modes [21]. These modes occur when longitudinal and shear wave reflections constructively interfere and energy propagates through the plate [21]. Several methods have been proposed to enhance the interpretation of the measured Lamb wave signals to detect and locate structural damage. They are based on changes in wave attenuations using wavelets [9,22], time-frequency analysis [10], wave reflections [7], and time of flight information [23]. A more complete description on the Lamb wave propagation technique can be found in the references [9,24]

Monitoring pipe structures using Lamb waves is complicated by several factors. Generating a single, pure mode for a pipe structure is difficult because of the presence of multiple modes at each frequency [25], whereas an isotropic plate structure has only two distinct modes, symmetric and anti-symmetric, present at lower frequencies. Nomenclature for the three classes of tube modes present in hollow cylinder wave guides are outlined by Silk and Bainton [21], then modified by Demma, et al. [26] for their software, referred to as *Disperse*. The three types of modes are as follows: Longitudinal axially symmetric modes *L(0,n)*; Torsional axially symmetric *T(0,n)*; and Non-axially symmetric (Flexural) modes *F(m,n)*. The first two classes correspond to modes in a flat plate. For this notation, *m* represents the harmonic number of circumferential

variation and n is an index counter [26]. Another difficulty with Lamb wave techniques, in general, is that the modes are dispersive. The shape of the propagating wave will change with distance which makes interpretation of results somewhat difficult [25].

Recent research works [4,5,25,26,27] have shown significant successes in pipeline damage identification using Lamb wave propagations. These techniques use a pulse-echo transducer arrangement, where arrival times and changes in signal amplitude at reflection are used to indicate the presence and location of defects [28]. Although these methods provide commercially viable monitoring products using Lamb wave propagations as a tool for damage detection, they require relatively sophisticated instruments and direct access to the surface of the pipeline. The transducers used in these studies are attached to the exterior surface of a pipe in a ring consisting of independent transducers distributed evenly about the pipe's circumference. These methods, however, are problematic if the pipe is underground or the pipe is covered by insulating layers.

For this research, the Lamb wave technique was examined with the use of directional MFC patches instead of a dry-coupled PZT ring transducer assembly. As discussed in the introduction, the advantages of using MFC patches are the flexibility of the patch allowing direct mounting to the curved surface of the pipe, inexpensive fabrication methods that reduces overall cost of the sensors, and the directionality of the signal generation by a ring of MFC patches that excites asymmetric modes while minimizing flexural modes. These MFC sensors could be installed directly into the surface of pipelines in difficult to reach area, and monitor the condition of the structure, realizing the concept of on-line structural health monitoring.

3. EXPERIMENT

3.1 Pipeline Structure

The apparatus used for the experimental procedures was a simple pipeline consisting of three steel pipe sections. The three sections were connected together using two flanged joints to form a continuous, straight pipeline, as seen in Figure 1. The middle pipe section was 2.1-m long, and each of the end pipe sections was 0.9-m long, making the entire apparatus 3.9-m long. Each flanged joint connected using four bolts (9.5-mm), and each bolt was originally tightened with a torque wrench to 22.6-N-m. Each of the three pipe sections was made of the same type and size of carbon steel tubing. The pipe sections had an outer diameter of 6.4-cm and a wall thickness of 1.60-mm. The pipe was suspended using elastic cords which were looped around the pipe near each of the ends of the overall pipeline structure.

Several MFC patches were used to monitor the condition of the pipeline structure. The MFC provides large flexibility that allows easy integration into the pipeline. Traditional piezoceramic materials were not suitable for this application, as confirmed by previous studies [29]. The patches have an active area of 85-mm x 57-mm with overall dimensions 110-mm x 75-mm (Smart-Materials, Inc., M8557). MFC patches were located at five axial locations along the length of the pipeline structure. Details of the actual locations of the MFC patches are shown in Figure 2. The first two axial locations were 64-mm from each side of flange A, and the second two locations were 64 mm from each side of flange B. At each of the axial locations, a single MFC patch was mounted to the pipe's exterior surface. The MFC patches at the first three axial locations were mounted at the same circumferential location, but the MFC patch at the fourth

axial location was mounted on the opposite side (180° around the circumference) from the other three. An example of the mounted patches can be seen in the Figure 3.

In order to make a pulse-echo Lamb wave measurement from the axial location close to flange B, seven additional MFC patches were mounted around the circumference of the pipe. Because of space constraints, three of the patches were mounted in a ring with the existing patch at the axial location that was used for impedance measurements, and the remaining four patches were mounted in a ring directly next to the first ring, as seen in the Figure 2. Therefore, two circumferential rings of MFC patches were used to make the pulse-echo measurements. One ring was used as the actuator and the other as the sensor. Because the two rings were mounted at nearly the same axial location, the measurement was considered pulse-echo rather than pitch-catch. The patches were bonded to the metal surface of the pipe using epoxy, which was allowed to cure in a vacuum bag for 12 hours at a gauge pressure of 1.02-atm.

3.2 Experimental Procedure

3.2.1 Impedance Method

The impedance method is used to monitor the conditions of the connection joints in flanges. For the impedance measurements, four MFC patches from each located at 2, 3, 4, and 5 in Figure2, were used. An Agilent 4294 impedance analyzer was used for the data acquisition. Two frequency ranges were used for the measurements: 50-60 kHz and 110-120 kHz. The sensitivity of the vibration-based NDE techniques in detecting damage is closely related to the frequency band selected. To sense incipient-type damage, it is necessary for the wavelength of excitation to be smaller than the characteristic length of the damage to be detected [30] In order to ensure high sensitivity to incipient damage, the electrical impedance is measured at high frequencies in

the range of 30 kHz to 400 kHz. Under this high frequency range, the wavelength of the excitation is small, and sensitive enough to detect minor changes in the structural integrity. At frequencies greater than 30 kHz, the dynamic response of a host structure is usually limited to local areas surrounding the MFC patch. Additionally, high frequency excitation allows measurements obtained by the MFC patch to be insensitive to far-field conditions such as operational vibrations and boundary condition changes. Another advantage of this limited sensing area is that the method not only detects the presence of damage but can also pinpoint which flange is damaged. For both frequency ranges, 801 data points were taken. A 1-V swept sine wave was used for the excitation. Four averages were made per point, and only one complete sweep was used.

All impedance data were taken in sets. A set of data contained eight ensembles. Each of the eight ensembles involved measuring the impedance of a given MFC patch for one of the two frequency ranges. Therefore, the use of four MFC patches and two frequency ranges corresponded to eight ensembles of data per data set. Five sets of baseline measurements were taken. The purpose of the baseline measurements was to provide a means of comparison between the undamaged and the simulated damaged conditions of the pipeline structure. The baseline measurements were taken at various times over the course of three days. As will be shown later, the variation in the baseline measurements was minimal compared to the variation caused by structural damage. It should be noted that the measurement taken over three days may not be able to accommodate a significant environmental condition changes with the limitation of the laboratory setting, however, it was done in an effort to confirm the repeatability of the

measurement and possibly capture any malfunction of sensors and data acquisition systems. The performance of the impedance method under a large temperature variation, please refer [31].

After the completion of baseline measurements, damage cases were introduced. Each damage case involved removing one or more bolts from a particular flange in an effort to simulate loosening of the flanged joint. Primary concentration was made with the damage to flange A, the results from which are presented in this paper. However, a limited number of damage cases with flange B were also implemented to verify that the proposed methods correctly identified the location of the damage. A loosening mode of bolted joints in flanges was chosen in this study as it could easily be implemented using a torque wrench. The loosening of bolts was also reversible so that multiple damage measurements could be made without permanently altering the apparatus.

With the damage to flange A, three different damage cases were used to demonstrate the ability of the proposed methods to detect, locate, and quantify the damage present. For the first damage case, bolt #1 was removed from flange A (see Figure 2). For the second damage case, bolt #2 was also removed. Because the pipeline structure was suspended by elastic cords near each of its ends, the weight of the pipeline placed the loosened part of the joint under compression. Therefore, damage case three had the same bolts removed as damage case two (bolt #1 and bolt #2 from flange A), but the pipe was rotated circumferentially by 180° so that the weight of the pipeline placed the loosened part of the joint under tension. For each of the damage cases, three sets of data were taken at different times in the day.

3.2.2 Lamb Wave Method

For the Lamb wave measurements, two circumferential rings of four MFC patches each were used. The two rings were located at axial locations 1 and 3. In other words, only MFC patches *1a*, *1b*, *1c*, *1d*, *3a*, *3b*, *3c*, and *3d* were used. A portable data acquisition system was used to generate the input waveform and measure the subsequent traveled waves. The waveform was first amplified by an external power amplifier. The amplified waveform was then simultaneously input to the four MFC patches at axial location 3. The four MFC patches at axial location 1 were then used to simultaneously measure the response. The response signals were then stored for analysis.

As described in the previous section, Lamb wave propagation in cylindrical structures is much more complicated than plate-like structures. As shown in Figure 4, multiple modes exist at any given frequency. Figure 4 is a group velocity dispersion curve of the test apparatus generated by *PCDISP* software [32]. To successfully use Lamb wave propagation as a tool for detecting and locating structural damage in pipelines, the excitation frequency must be chosen carefully. Ideally, a single mode would be excited so that the measured responses would be easily identified and interpreted.

For this experiment, mode L(0,2) is chosen as the best candidate for excitation because of its relatively non-dispersive group velocity characteristic over a large frequency range [25]. As shown in Figure 4, mode L(0,2) is the fastest of the modes in the frequency range higher than 50 kHz. The L(0,2) mode will arrive at the MFC sensor first and can be separated from other signals

if a time-domain gating window is used. A 70-kHz frequency is selected from the group velocity curve because L(0,2) had good separation from F(1,3) and other modes.

A burst waveform was chosen as an input waveform. The input was created by applying a Gaussian window to a 5-cycle sine wave. Once baseline measurements of the pipeline were recorded, damage was simulated by attaching two pipe clamps to the structure. The clamps were located 1.04-m from flange *A2*. This reversal damage was first considered in this study to assess the performance of the MFC as a pipeline Lamb wave transducers. The Lamb wave measurements were repeated after introducing the damage.

4. EXPERIMENTAL RESULTS AND ANALYSIS

4.1 Impedance Method

An example of an impedance measurement is shown in Figure 5. This figure shows the entire frequency range used in the frequency measurement of 50-60 kHz. The impedances in this figure were taken from the MFC at the axial location #2, which is located closest to flange A. Only the real portion of the electrical impedance was analyzed to predict damage because it is more sensitive to structural changes than the imaginary part. The third damage case is plotted in comparison to a baseline measurement. With induced damage, certain changes in peaks and shapes of the impedance spectrum are clearly observed.

A view of the impedances over a narrower frequency range, 51-53 kHz, with the baseline measurement and the first three damage cases can be seen in Figure 6. It can be seen in the figure that as damage increases, corresponding changes in impedance are observed. However, it

is difficult from such a plot to quantify the degree to which the structure is damaged. In order to quantify the change in the impedance signature caused by damage, a damage metric is calculated.

The damage metric used here was formulated using the cross correlation coefficient between a particular damage case and the first baseline measurement. The correlation coefficient determined the linear relationship between the two data sets. The formulation of the correlation coefficient of a normalized difference between the baseline and current measurements is given by the following:

$$\rho = \frac{1}{n-1} \frac{\sum_{i=1}^{n} (\mathrm{Re}(Z_{i,1}) - \mathrm{Re}(\overline{Z}_1))(\mathrm{Re}(Z_{i,2}) - \mathrm{Re}(\overline{Z}_2))}{\sigma_{Z_1} \sigma_{Z_2}} \qquad (2)$$

where ρ is the correlation coefficient, $Z_{i,1}$ is the baseline impedance data and $Z_{i,2}$ is the compared impedance at frequency i, $\overline{Z}_1$ and $\overline{Z}_2$ are the means of the signals and the σ terms are the standard deviations. For convenience, the feature examined in this case is typically $(1-\rho)$, which is done merely to ensure that the damage metric values increase with increasing damage or with increasing change in structural integrity. Therefore, a damage metric value of zero, when compared to a baseline measurement, corresponds to perfect correlation. Perfect correlation between a given measurement and a baseline measurement, in turn, means that there is no damage present for that given measurement. A greater damage metric value means that a certain degree of dissimilarity, with respect to a baseline measurement, is present in a particular measurement. In addition, an increase in the value of the damage metric corresponds to an increase in this dissimilarity. The goal here is to show that this dissimilarity is directly related to the amount of damage present.

The damage metric for the 50 to 60-kHz range for each damage cases is shown in Figure 7. Similarly, the damage metrics for the higher frequency ranges (110 to120-kHz) are shown in Figure 8. All of the metric values were normalized by dividing them by mean of the five baselines because the relative change, rather than absolute value, was of primary concern in this study. This procedure minimizes the impact of different bonding conditions between a MFC patch and the structure, which may cause relatively large variations in baseline and subsequent test measurements.

From the figures, one can clearly see that the damage metric is effective at detecting the presence of damage in the structure. For the MFC patches closest to the damage location (axial location #2 and #3), the damage metric was at least an order of magnitude greater for all damage cases than it was for any of the baseline measurements. As mentioned above, the variation shown in each of the five baseline measurements was insignificant compared to the variation caused by damage.

In addition, the results shown in Figure 7 and 8 can be used to make a clear decision regarding the damage location and its quantification. The impedance measurements for both frequency ranges were effective at locating the damage in the system. For damage case 1, the damage metrics at axial locations #2 and #3 were nearly twenty times greater than the corresponding damage metric for the baseline measurements. Note that these two axial locations were the nearest to where the damage was located (flange A) than the other two axial locations. On the other hand, the damage metrics for case 2 at axial locations #4 and #5 showed only relatively

slight increases over the corresponding damage metric for the baseline. In fact, axial location #5 showed almost no relative difference between the baseline and damage measurements at 110- to 120-kHz. This lower value in the relative damage detected could be attributed to the fact that axial location #5 was on a completely different section of pipe than axial location #4. Therefore, axial location #5 showed less change from the presence of damage than axial location #4.

From the results at axial location #4 for both frequency ranges, the higher frequency range demonstrated a more localized sensitivity to damage compared to the lower frequency range. For each of the damage cases, the damage metric at axial location #4 was at least 25% lower for the higher frequency range than the lower frequency range. The results also show that the impedance measurements for both frequency ranges were effective at quantifying the amount of damage in the system. In each instance, the damage metric increased in value as the corresponding level of damage increased, which can be clearly observed by the results at axial location 1. Therefore, the structural damage to the bolted joints of the flanges could be detected, located, and somewhat quantified with the use of the impedance methods utilizing MFC tranducers.

To demonstrate that the impedance method correctly located the damage, a fourth and final damage case was implemented. This case involves damage to the opposite flange from the previous damage cases. For this damage case, the pipe was first returned to the conditions of damage case 2 by again circumferentially rotating the pipe 180° and leaving bolts #1 and #2 removed. The weight of the pipe was again placing the damage at flange A under compression. Without replacing the two bolts from flange A, the fourth damage case was then implemented by

removing bolts #1 and #2 from flange B. Therefore, a total of four bolts were absent, two from flange A and two from flange B.

As with the previous damage cases, two impedance measurements were taken for each frequency range, 50 to 60-kHz and 110 to 120-kHz. The damage metrics for damage case 4 at each axial location for the lower frequency range (50 to 60-kHz) are shown in Figure 9. Because the two bolts were left out of flange A, the damage metric for damage case 2 was repeated in this figure. Similarly, the damage metrics for the higher frequency range (110 to 120-kHz) are shown in Figure 10.

From the damage metrics in Figures 9 and 10, the proposed methods correctly identified the additional damage at flange B. For both frequency ranges, the MFC at axial location #5 showed a dramatic increase in the value of the damage metric with case 4 when compared to case 2. At the same time, the MFC at axial location #2 showed no increase in the damage metric with case 4 when compared to case 2. Although the changes are not as significant as at axial location #5, the damage metrics for axial location #3 and #4 showed slight increases as well.

4.2 Lamb Wave Method

The MFC patch at axial location #3 of the pipeline structure used in the previous section, as seen in Figure 2, was then used to make Lamb wave measurements. Pulse-echo measurements were used to identify the presence of damage and determine its location. Damage was simulated by attaching two pipe clamps to the structure. The clamps were located on the middle pipe section, 1.1-m from flange A.

When using pulse-echo measurements, a reflection feature can be used to detect and locate damage in a structure. Damage in a pipe, such as cracks and corrosion, causes a local change in the pipe's mass, stiffness, and damping. As Lamb waves propagate through a damaged section of the pipe, the local changes from the damage can cause a portion of the Lamb waves to reflect. If the reflection is strong enough to propagate back to the transducer ring, the reflection feature can be detected. The presence of damage at a given point in time is detected by comparing a current measurement with a baseline measurement which was taken under damage-free conditions. The comparison of the two signals can be used to identify reflections in a current measurement that are not present in the baseline measurement.

Once the presence of damage is identified, an effort can then be made to identify the location of the damage. Using the time history of the response signal from the damage case measurement, the approximate time of arrival of the reflection from the damage can be estimated. Given that the group velocity of the reflected mode is known from the analytical dispersion curves or from a previous experiment, the distance traveled by the mode can be estimated from the time that elapsed between the pulse excitation and the arrival of the reflection. Once the traveled distance is known, the location of the damage is then identified relative to the location of the transducer ring. In this case, the location of the damage was half the distance traveled by the reflected mode because the mode must travel the distance twice, first on the way to the damage location from the actuator and then returning to the sensor after reflecting from the damage.

The exact time of arrival of a given reflection is, however, generally difficult to determine. Typically, the reflection of a given mode from damage is on the same order of magnitude as the coherent noise present in the baseline signal. In addition, the relatively low voltage level of the response signals means that there is a less than desirable signal to noise ratio (random noise, rather than coherent noise). Therefore, advanced signal processing techniques were used to extract the differences between baselines and tested signals so that the damage could be correctly identified.

The technique used here involved the discrete wavelet transform and the Hilbert transform. First, the discrete wavelet transform was used to de-noise the response signals from the baseline and damage case measurements. The Morlet wavelet was used as the mother wavelet for the wavelet transform in this study. A range of scales was used to perform the wavelet transformation, and then the wavelet coefficients corresponding to the excitation frequency (70 kHz) were extracted, discarding all other frequency content. The use of the discrete wavelet transform significantly reduced the random noise present in a given response signal.

Because environmental changes, such as temperature variation, can create slight phase differences between the baseline and damage case measurements, the direct difference between the wavelet coefficients of each measurement did not lend itself well for comparison. Often, the signal differences attributed to the phase variations were much more significant than the actual amplitude differences present because of a reflection feature. To avoid this issue, the Hilbert transform of the wavelet coefficients was first used to find the envelope of each signal's wavelet

coefficients. Finally, the direct difference between the two signal envelopes was then used for the actual comparison of the baseline and damage case measurements.

The damage detection algorithm, along with the results obtained from several forms of permanent damage, including a saw cut, cracks and corrosion induced in the pipeline, is presented in a separate document [33]. Only simulated forms of damage are presented here as a demonstration that the same MFC patch, which was used to detect joint damage using the impedance method in the previous section, could now be used to detect corrosion damage to the main body of the pipe. Although the clamped condition is not real damage, it changes the local stiffness, which introduces the similar effects of structural damage. This procedure also allows repeated tests before actually damaging the structure.

The results of the pulse-echo measurements were analyzed using the damage detection algorithm described above. The results for the absolute difference and percent difference between the baseline and the tested signal are shown in Figure 11. The absolute difference here refers the algebraic difference in the envelope of the Hilbert transform of the wavelet coefficients between the baseline and the tested signal, while the percent difference is the percent difference between the measurements. As mentioned in the previous section, the primary mode of concern in the experiment is the L(0,2) mode. The boundary reflected wave is clearly seen at .75-ms with a good signal-to-noise ratio. One can also notice that some other modes exist. However, because they are much smaller in magnitude compared to the L(0,2) mode, their effects are negligible. The reflection from the pipe clamps was so strong that its presence was very apparent in the plot of the absolute difference between the time data of the baseline and damage case measurement.

The estimated time of arrival for the reflection from flange B was 0.76-ms, which corresponded to a group velocity of 5600-m/sec. The estimated time of arrival for the reflection from the damage was 0.37-ms. Using the group velocity and time of arrival for the damage reflection, the estimated location of the damage was 1.0-m from flange A, which was a 2.8% difference from the actual damage location. Therefore, this set of measurements demonstrated that the same MFC patch used for making impedance measurements to detect joint damage could also be used for Lamb wave measurements to detect damage in the main body of the pipe.

Because a portion of the initial signal was reflected from the damage location, the boundary reflected wave signal also decreased in amplitude when compared with the baseline measurement, as shown in Figure 11. Therefore, the wave attenuation feature could also be utilized to detect surface damage in pipeline structures. Although this feature is not able to locate the damage, the degree of attenuation of the boundary reflected wave can be used to estimate the size or severity of surface damage.

5. DISCUSSIONS

The impedance measurement presented here involved the use of MFC transducers to successfully detect and locate damage in flanged joints in pipelines. The same MFC patches used for impedance measures here were also used for detecting damage to the main body of the pipeline structure by employing Lamb wave propagations. The dual use of the MFC patches is extremely important to the success of the proposed monitoring methods. In order to monitor the structural health of both the joints and the body of the pipe, both impedance methods and Lamb wave

methods are required. The localized nature of impedance measurements makes them insensitive to cracks and corrosion damage located near the opposite end of the pipe. However, the method is very effective at monitoring damage to the bolted joints. On the other hand, Lamb wave measurements were insensitive to damage to the bolted joints at the flanges. However, the pulse-echo measurements show that they were very capable of detecting and locating cracks and corrosion damage along the entire length of the body of the pipe.

By implementing the flexible nature of MFC patches which enables them to be bonded directly to the curved surface of the pipe, the same set of transducers can be effectively used to evaluate both joint connection and corrosion damage. The importance of this approach cannot be over-emphasized. By enabling a single transducer to perform multiple tasks, the required number of transducers is reduced, which in turn reduces the cost to employ such a system. In addition, maintenance costs will decrease, and post-event assessments can occur rapidly using the proposed methods. Therefore, the entire monitoring process can be simplified with the application of MFC patches to pipeline structures.

While this method demonstrated great feasibility, there are still several research issues remaining for further investigation. Although the MFC could be easily installed on the pipe, it would be somewhat labor-intensive if one needs to apply relatively large numbers of sensors and actuators to miles of pipelines. Portable instrumentation using dry-coupled MFC patches, which facilitates the installation with much lower costs compared to the traditional ring-type of piezoelectric transducers, would remedy such problems. In addition, in order to maintain an optimal number of sensors and actuators, the sensing region of the impedance sensor and the traveling distance of

Lamb waves need to be more quantitatively assessed. Furthermore, the damage detection problem associated with if both surface and joint damage were spaced closely each other must be clearly addressed in the future studies. Finally, the implementation of automated signal processing techniques will improve the performance of the proposed technique and reduce the burden for analysts. All of the issues mentioned here are currently being addressed and will be the subject of subsequent papers.

6. CONCLUSIONS

An integrated approach for identifying structural damage in pipeline structures has been presented. The proposed SHM system relies upon the deployment of macro-fiber composite (MFC) patches for the entirety of the sensor array. Two damage detection techniques, guided Lamb waves and impedance methods, are implemented using the MFC patches, avoiding the necessity for two separate sensor arrays. Because MFC patches are flexible and resilient, they can be permanently bonded to the curved surface of a pipeline's main body. This permanent installation allows for the continuous monitoring of the pipeline system and reduces the costs associated with implementing NDE techniques, such as excavation to gain direct access to the pipeline. The impedance method was used to detect and locate connection damage in the flanged joints, in which Lamb wave methods are less sensitive. From the Lamb wave responses, the location of surface damage in main body of pipelines was identified by tracking wave attenuation and reflection information. Both methods operate at high frequency ranges, where there are measurable changes in minor defects in the pipeline structure. While future issues still remain, the research of this paper demonstrates the feasibility of implementing a low-cost, in-situ structural health monitoring system for pipeline systems.

7. ACKNOWLEDGEMENTS

The research was conducted at the Los Alamos National Laboratory, as a part of the 2004 Los Alamos Dynamics Summer School (LADSS). Funding for LADSS was provided by the Engineering Sciences & Applications Division at the Los Alamos National Laboratory and the Department of Energy's Critical Skills Programs Office. The following companies generously provided various software packages that were necessary to complete the projects: Vibrant Technologies (experimental modal analysis software), The Mathworks, Inc. (numerical analysis software), and Hibbitt, Karlsson and Sorensen, Inc. (ABAQUS finite element software). The authors would also like to acknowledge Dr. Charles Farrar, the director of LADSS, for organizing the School and providing his expert advice on this project.

REFERENCES

[1] Posakony, G.J., Hill, V.L., (1992). "Assuring the Integrity of Natural Gas Transmission Pipelines." *Topical Report, GRI*, Nov. 1992.

[2] National Transportation Safety Board, (2000). "Natural Gas Pipeline and Fire Near Carlsbad, New Mexico, August 19, 2000" *Pipeline Accident Report NTSB/PAR-03/01*, 1-57, Washington, D.C.

[3] National Transportation Safety Board, (1999). "Pipeline Rupture and Subsequent Fire in Bellingham, Washington, June 10, 1999" *Pipeline Accident Report NTSB/Par-02/02*, 1-79, Washington, D.C.

[4] Lowe, M.J.S., Alleyne, D.N., Cawley, P. "Defect Detection in Pipes Using Guided Waves." *Ultrasonics* 36 (1998): 147-154

[5] Barshinger, J., J. L. Rose, M. J. Avioli, Jr. "Guided Wave Resonance Tuning for Pipe Inspection." *Journal of Pressure Vessel Technology*. Vol. 124, No. 3: 303-310, August, 2002.

[6] Park, G., Sohn, H., Farrar, C.R., Inman, D.J. (2003). "Overview of Piezoelectric Impedance-based Health Monitoring and Path Forward," *The Shock and Vibration Digest,* **35**, 451-463.

[7] Giurgiutiu, V., Zagrai, A., Bao, J.J. (2002). "Piezoelectric Wafer Embedded Active Sensors for Aging Aircraft Structural Health Monitoring," *International Journal of Structural Health Monitoring*, **1**, 41-61.

[8] Bhalla, S., Soh, C.K., (2004). "High Frequency Piezoelectric Signatures for Diagnosis of Seismic/Blast Induced Structural Damages," *NDT&E International*, **37**, 23-33.

[9] Kessler, S.S., Spearing, S.M., Soutis, C., (2002). "Damage Detection in Composite Materials using Lamb Wave Methods," *Smart Materials and Structures*, **11**, 269-278

[10] Ihn, J.B., F.K. Chang, F.K., (2004). "Detection and monitoring of hidden fatigue crack growth using a built-in piezoelectric sensor/actuator network: II. Validation using riveted joints and repair patches," *Smart Materials and Structures,* **13**, 621-630.

[11] Giurgiutiu, V., Zagrai, A., Bao, J.J., (2004). "Damage Identification in Aging Aircraft Structures with Piezoelectric Wafer Active Sensors," *Journal of Intelligent Material Systems and Structures*, **15**, 673-688.

[12] Wait, J.R., Park, G., Farrar, C.R., (2004). "Integrated Structural Health Assessment using Piezoelectric Active Sensors," *Shock and Vibration*, **12**, 389-405.

[13] W.K. Wilkie, R.G. Bryant, J.W. High, R.L. Fox, R.F. Hellbaum, A. Jalink, B.D. Little, and P.H. Mirick, "Low-Cost Piezocomposite Actuator for Structural Control Applications,"

Proceedings of 7th SPIE International Symposium on Smart Structures and Materials, Newport Beach, CA, March 5-9, 2000.

[14] Sodano, H.A., Park, G., Inman, D.J., 2004, "An Investigation into the Performance of Macro-Fiber composites for Sensing and Structural Vibration Applications," *Mechanical Systems and Signal Processing*, **18**, 683-697.

[15] Park, G., Farrar, C.R., Rutherford, C.A., Robertson, A.N., 2004, "Piezoelectric Active Sensor Self-diagnostics using Electrical Admittance Measurements," *ASME Journal of Vibrations and Acoustics*, in press.

[16] Simmons, W.C., (1986) "Bolt Failure Studies at Aberdeen Proving Ground", Analyzing Failures: Problems and Solutions, *Presented at Intern Conf and Exp on Cracks and Fatigue, Corrosion and Cracking, Fracture Mechanics and Failure Analysis*, Salt Lake City, UT, 1986.

[17] Eidinger, J.M., "Girth Joints in Steel Pipelines subjected to Wrinkling and Ovalling," *Proceedings, 5th U.S. Conference on Lifeline Earthquake Engineering.* 1999:100-109.

[18] Sun, F P., Chaudhry, Z., Liang, C., Rogers, C.A. (1995), "Truss Structure Integrity Identification Using PZT sensor-actuator." *Journal of Intelligent Material Systems & Structures,* **6**, 134-139.

[19] Park, G., Farrar, C.R., Rutherford, C.A., Robertson, A.N., (2006), "Piezoelectric Active Sensor Self-diagnostics using Electrical Admittance Measurements," *ASME Journal of Vibration and Acoustics*, 128, 469-476.

[20] Park, G., Farrar, C.R., Lanza di Scalea, F., Coccia, S., (2006) "Performance Assessment and Validation of Piezoelectric Active Sensors in Structural Health Monitoring," *Smart Materials and Structures*, **15**, 1673-1683

[21] Silk, M. G., Bainton, K.F. (1979) "The propagation in metal tubing of ultrasonic wave modes equivalent to Lamb waves." *Ultrasonics,* **27**, 11-19.

[22] H. Sohn, G. Park, J.R. Wait, N.P. Limback, C.R. Farrar, Wavelet-based Signal Processing for Detecting Delamination in Composite Plates, *Smart Materials and Structures*, **13** (2004), 153-160.

[23] M. Lemistre, D. Balageas, Structural Health Monitoring System based on Diffracted Lamb Wave Analysis by Multiresolution Processing, *Smart Materials and Structures*, **10** (2001), 504-511.

[24] N. Bourasseau, E. Moulin, C. Delebarre, P. Bonniau, Radome Health Monitoring with Lamb Waves: Experimental Approach, *NDT&E International,* **33** (2000), 393-400.

[25] Alleyne, D. N., Lowe, M., Cawley, P. (1998). "The Reflection of Guided Waves From Circumferential Notches in Pipes." *Journal of Applied Mechanics,* **65**, 635-641.

[26] Demma, A., Cawley, P., Lowe, M., Roosenbrand, A.G. (2003). "The Reflection of the Fundamental Torsional Mode from Cracks and Notches in Pipes." *Journal of Acoustic Society of America,* **114**, 611-625.

[27] Alleyne, D.N., Pavlakovic, B., Lowe, M., Cawley, P. (2001) "Rapid long-range inspection of chemical plant pipework using guided waves." *Insight,* **43**, 93-96.

[28] Lowe, M., Alleyne, D.N., Cawley, P. (1998). "The Mode Conversion of a Guided Wave by a Part-Circumferential Notch in a Pipe." *Journal of Applied Mechanics,* **65**, 649-656.

[29] Park, G., Cudney, H., Inman, D.J., (2001), "Feasibility of Using Impedance-based Damage Assessment for Pipeline Systems," *Earthquake Engineering & Structural Dynamics Journal*, **30**, 1463-1474.

[30]Stokes, J. P., and Cloud, G. L., (1993) "The Application of Interferometric Techniques to the Nondestructive Inspection of Fiber-reinforced Materials", *Experimental Mechanics*, **33**, 314-319.

[31]Park, G., Kabeya, K., Cudney, H., Inman, D.J., (1999) "Impedance-based Structural Health Monitoring for Temperature Varying Applications," *JSME International Journal*, **42**, 249-258.

[32] Seco, F., Martin, J.M. Jimenez, A., Pons, J.L, Calderon, L., and Ceres, R. "PCDISP: A Tool for the Simulation of Wave Propagation in Cylindrical Waveguides." *Proceedings of ninth International Congress on Sound and Vibration, Orlando*, Florida (2002).

[33] Thien, A.B., 2006. *Pipeline Structural Health Monitoring using Macro-Fiber composite Active Sensors* M.S. Thesis, University of Cincinnati.

List of Figures

List of Tables

Figure 1: Apparatus for testing

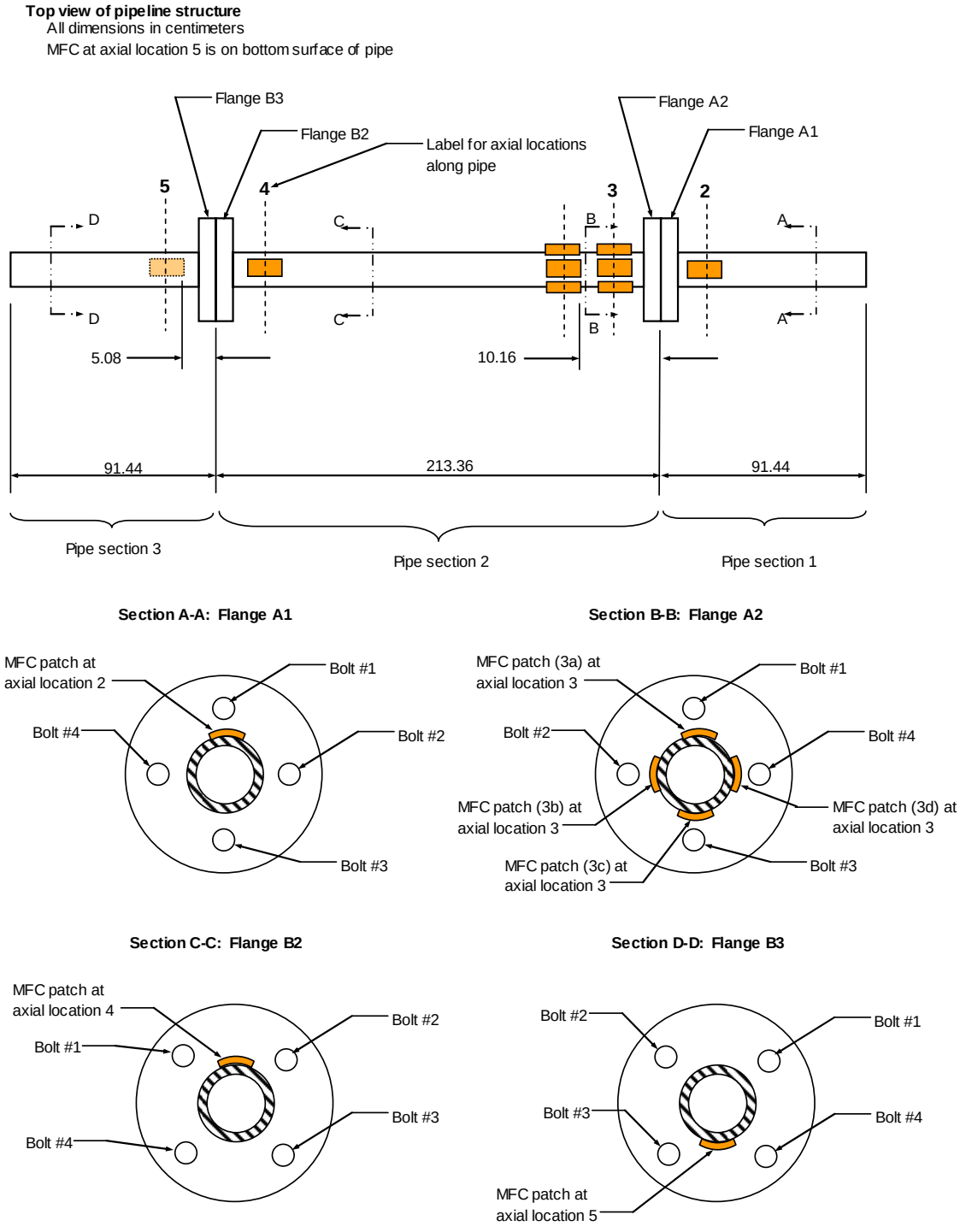

Figure 2: Dimensioned drawing pipeline structure, including flanged joints

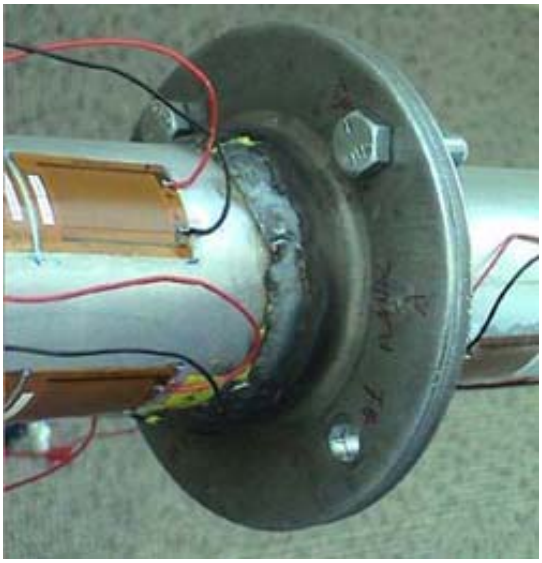

Figure 3: Example MFC patch bonded on the surface of Pipe

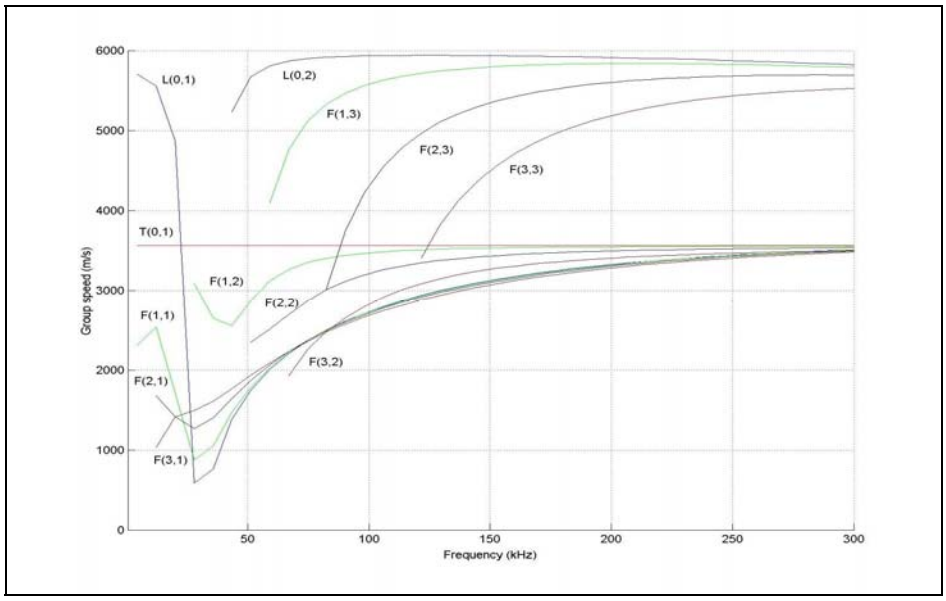

Figure 4: Group velocity curves for pipeline structure

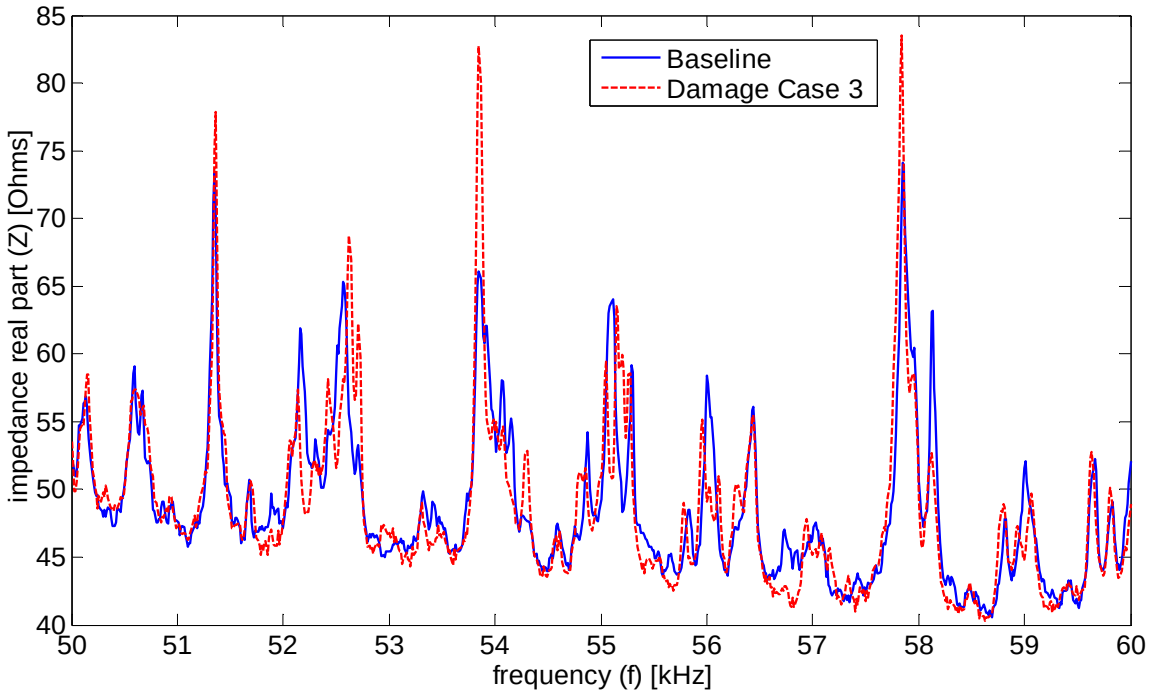

Figure 5: Comparison of baseline and damage-case 3 impedances (50 to 60-kHz)

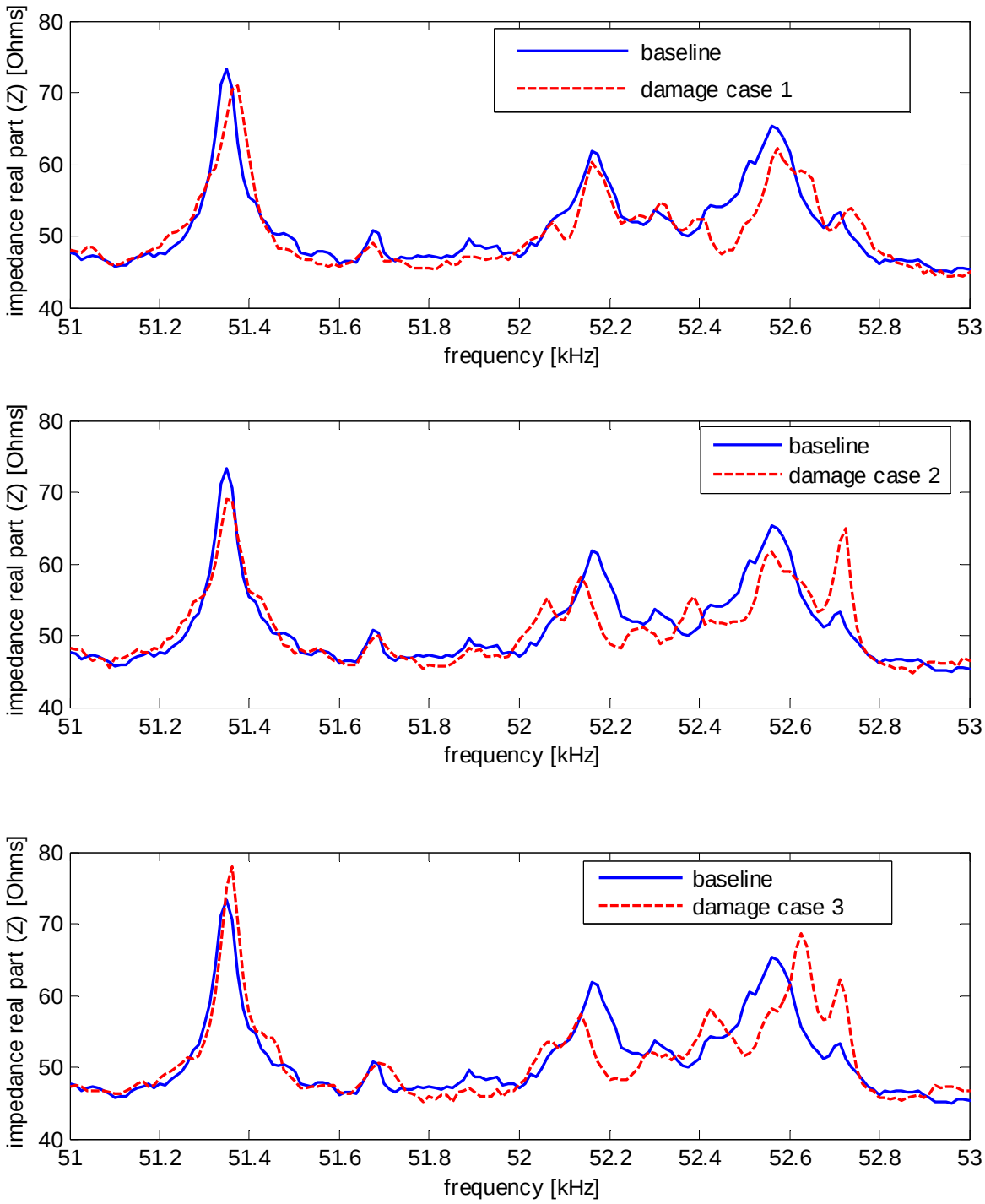

Figure 6: Comparison of baseline and damage-case impedances (51 to 53-kHz)

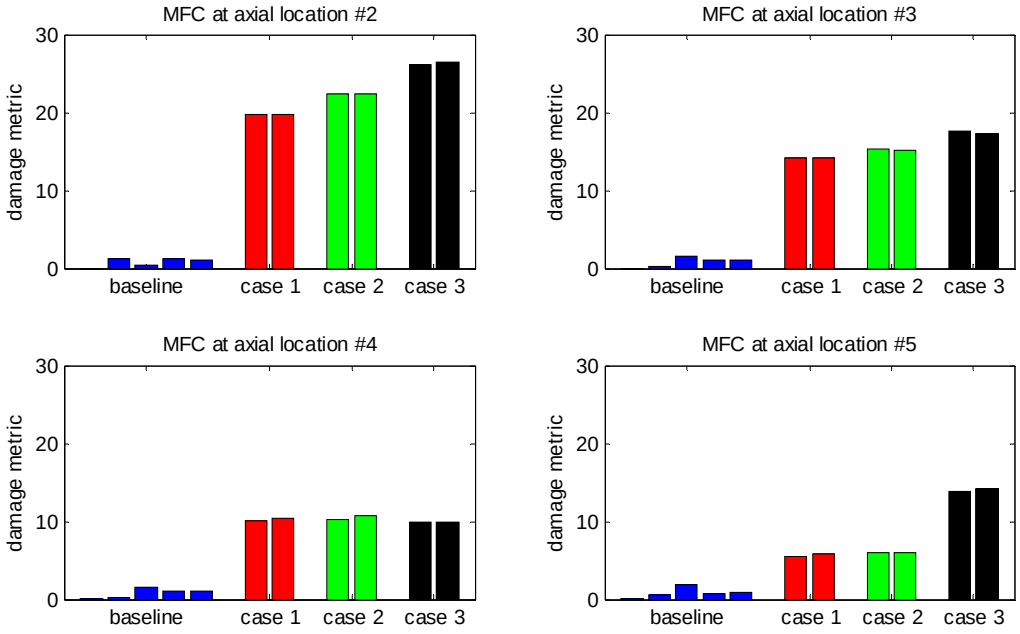

Figure 7: Damage metric for damage to flange A (50 to 60-kHz)

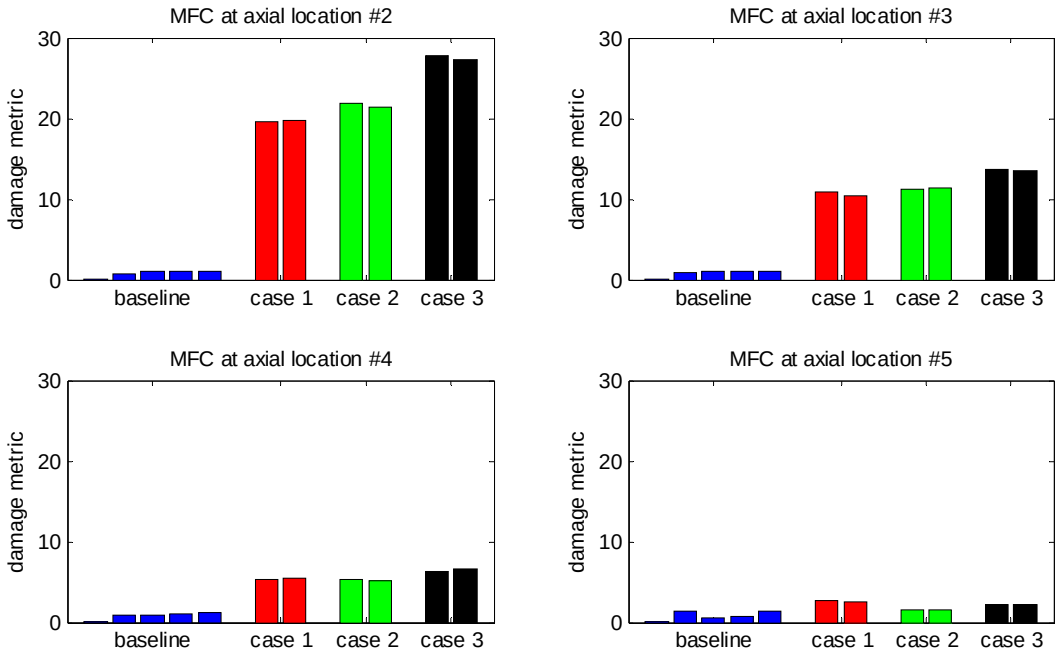

Figure 8: Damage metric for damage to flange A (110 to 120 kHz)

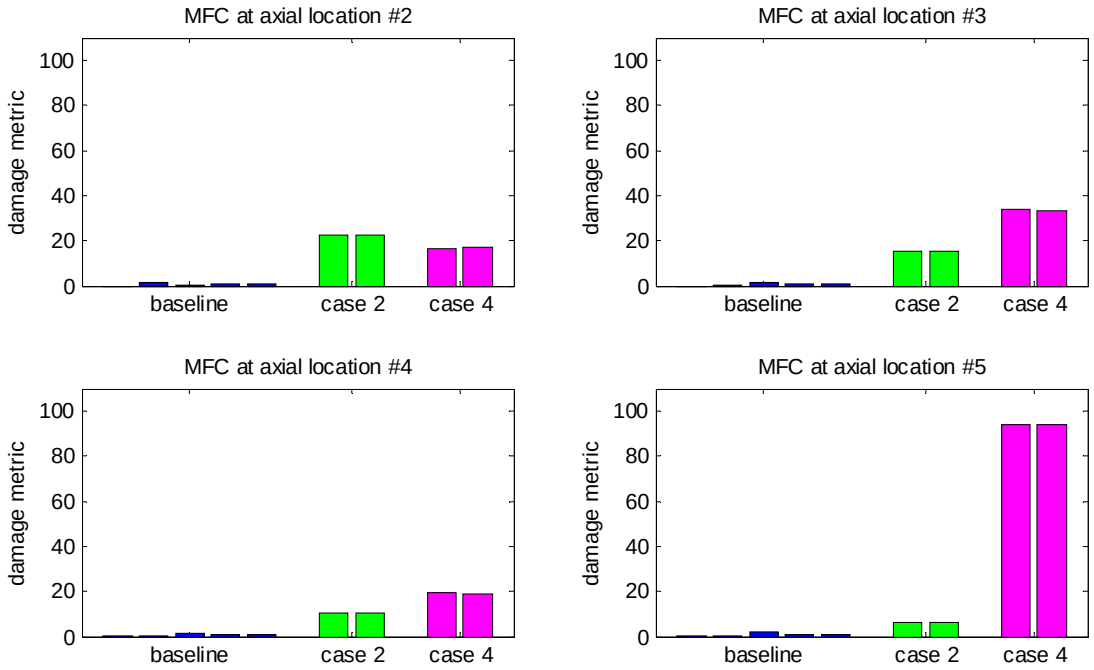

Figure 9: Damage metric for damage to flange B (50 to 60-kHz)

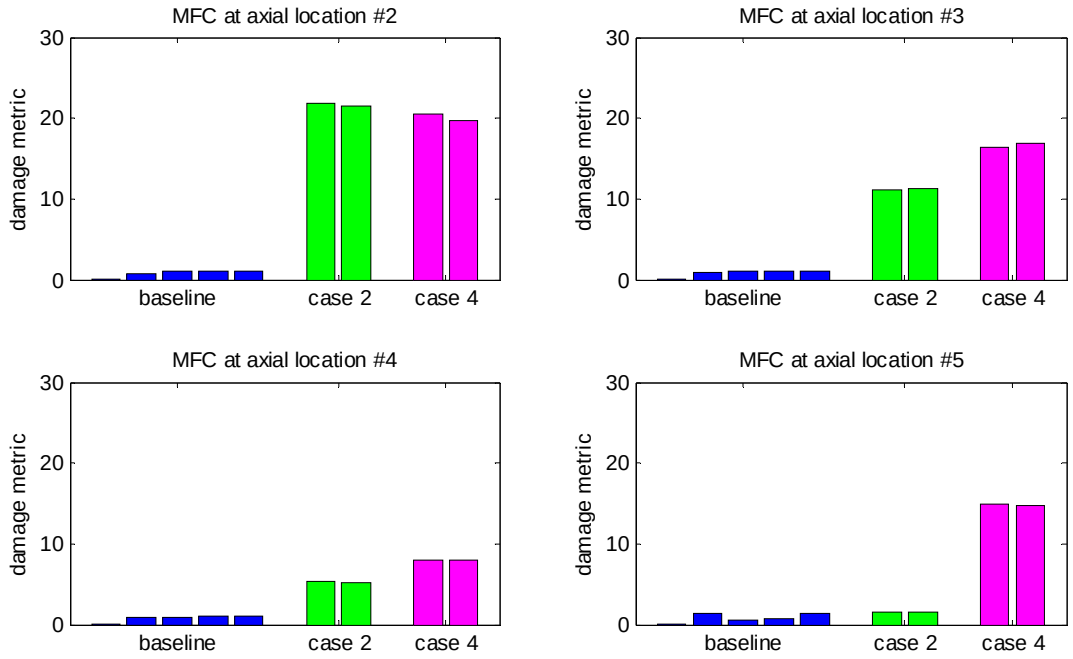

Figure 10: Damage metric for damage to flange B (110 to 120-kHz)

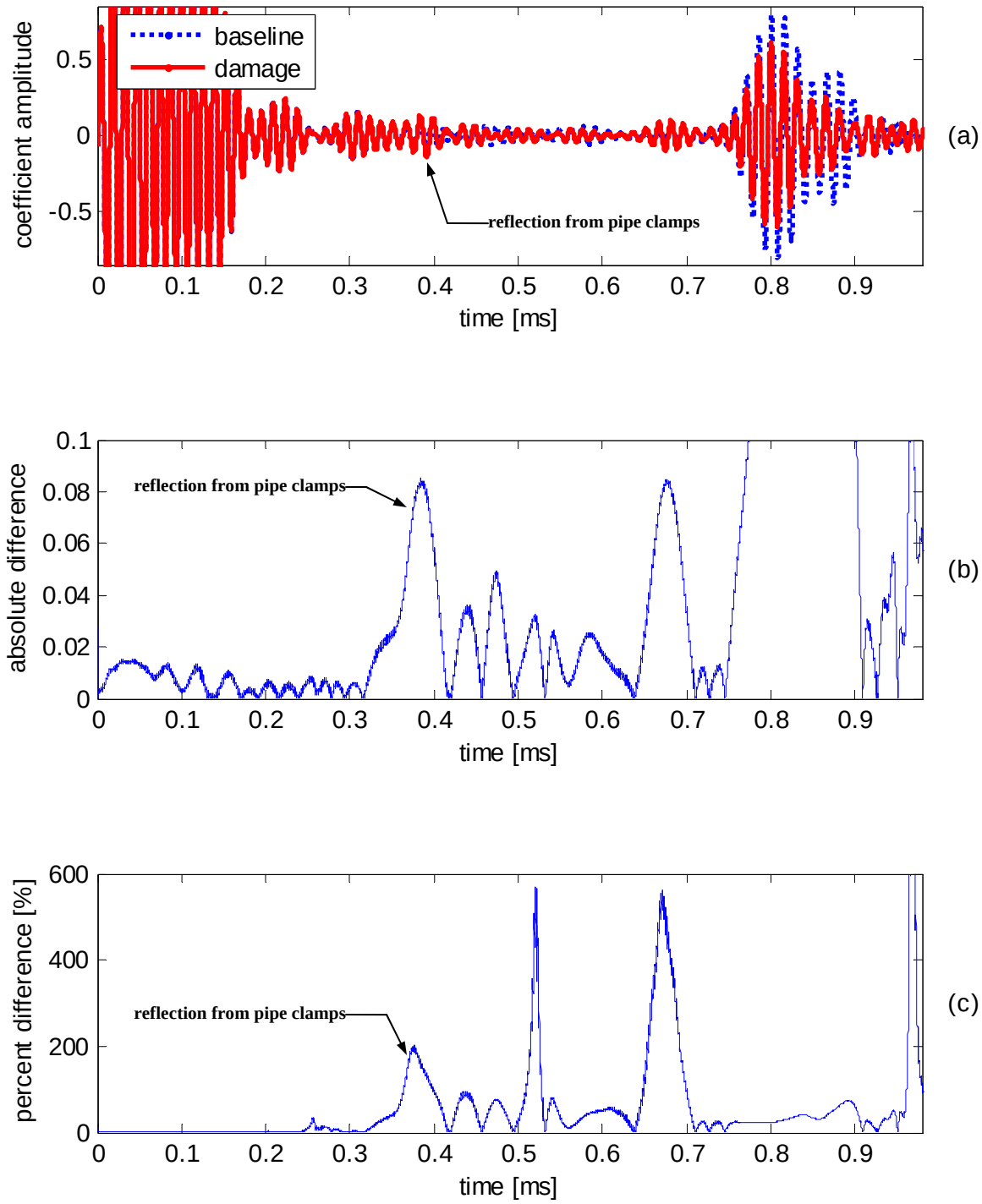

Figure 11: (a) Time history for a damage-case (2 pipe clamps) and a baseline measurement, (b) difference between the signal envelopes (c) percent difference between the signal envelopes